Deformation Evaluation and Displacement Forecasting of Baishuihe Landslide after Stabilization based on Continuous Wavelet Transform and Deep Learning

Yuting Liu
UNIPD DICEA: Universita degli Studi di Padova Dipartimento di Ingegneria Civile Edile e Ambientale
Giordano Teza
Alma Mater Studiorum Universita di Bologna: Universita degli Studi di Bologna
Lorenzo Nava
UNIPD: Universita degli Studi di Padova
Zhilu Chang
UNIPD: Universita degli Studi di Padova
Min Shang
summing@126.com

China Three Gorges University
Debing Xiong
SGIDI Engineering Consulting(Group) Co., Ltd
Simonetta Cola
UNIPD DICEA: Universita degli Studi di Padova Dipartimento di Ingegneria Civile Edile e Ambientale

Research Article

Keywords: Landslide displacement forecast, Reservoir water level, Rainfall, Deep learning, DWT, CWT, CNN

Posted Date: May 17th, 2023

DOI: https://doi.org/10.21203/rs.3.rs-2691112/v1

Version of Record: A version of this preprint was published at Natural Hazards on April 21st, 2024. See the published version at https://doi.org/10.1007/s11069-024-06580-7.

Abstract

Baishuihe Landslide is a large active landslide that threatens shipping transportation in the Three Gorges Reservoir (China). A manual monitoring system has been active since 2003. However, after the realization of some intervention works in 2018-2019, new automatic instruments providing continuous data on displacements, rainfall, reservoir water level, and groundwater table were installed. The data recorded by the new system show that these works led to an effective stabilization improvement since the present displacement rate is lower than that detected before interventions. However, the relevance of the Three Gorges basin and the potential hazard of a possible collapse requires a reliable forecast of the landslide evolution in a time scale from a few hours to a few days. To this aim, a two steps procedure is here proposed. In the first step, after a preliminary preprocessing-denoising of data, carried out by means of Discrete Wavelet Transform (DWT), a Continuous Wavelet Transform (CWT) procedure is used to provide scalograms of the time series of three quantities, e.g., landslide displacement rate, rainfall and the difference of water level between the piezometer and reservoir water level. In the second step, to evaluate the relationships among the velocity trend and the other significant quantities and obtain a reliable velocity forecast, the images given by binding together two or three scalograms of the mentioned quantities were analyzed with a Convolutional Neural Network (CNN) tool. Several trials with different combinations of input time series of 2 or 3 quantities were carried out in order to recognize the factors which mainly affect the current displacement evolution. The results show that, after the works, rainfall is an important factor inducing deformation acceleration. The hydrodynamic pressure induced by the difference between the ground water pressure and reservoir water level also plays a dominant role in accelerating the Baishuihe landslide. Furthermore, the coupling of rainfall and hydrodynamic pressure produces displacement velocities higher than what the quantities singularly do. These results provide valuable indications for optimizing the monitoring configuration on the landslide and obtaining velocity forecasts in a few hours/days.

1. Introduction

Baishuihe landslide is one of the landslides activated with the impoundment of the Three Gorges Reservoir. It is a large-scale deep-seated landslide deforming all the time (Li et al. 2009; Miao et al. 2016). Its possible failure poses threats to the coastal buildings and facilities, also to people safety (Xu et al. 2018). Moreover, because of its acceleration, channel warnings and closures affect the shipping transportation causing substantial economic losses. In relation to the above, it is vital to ensure the stability of the Baishuihe landslide as much as possible, but also maintain an efficient monitoring system and improve the analysis of compiled data to increase the knowledge and improve the reliability of the landslide evolution forecasting.

The manual monitoring system, active since 2003, showed a regular displacement trend with a "step-like" shape once a year (Du et al. 2012). Since the magnitude of the "step-like" displacement tended to increase, some intervention works were conducted from October 2018 to October 2019. Meanwhile, the monitoring system was upgraded and converted to an automatic quasi-continuous acquisition of

displacements, rainfall and water level. The data obtained by the newly-built monitoring shows that the landslide significantly changed its displacement trend, becoming more stable. According to qualitative analysis, the periodical acceleration seems to be caused by rainfall. However, literature shows that the periodic water level fluctuation in the Three Gorges Reservoir is one of the main factors affecting the evolution of landslides in the area (Miao et al. 2020; Song et al. 2018). Hence, it is necessary to quantitatively analyze the factors that directly and potentially affect the displacement trend. Apart from this, displacement forecast is treated as an effective way to provide the basis for early warning. In this specific case, it is meaningful for forecasting the displacement evolution after stabilization.

In recent years, many mathematical and computational methods, such as statistical regression, machine learning and deep learning methods (Tehrani et al. 2022; Wang et al. 2022) were applied to landslide analysis. These methods are effective in many areas, including research on landslide forecasting (Ahmad et al. 2019). In this subject, many factors that induce landslides were considered. For instance, Orland et al. (2020) used soil moisture, pore pressure, and rainfall data to construct a deep learning model to predict the timing and magnitude of hydrologic response at multiple soil depths for the 36-hr interval for landslide-prone hillslopes in Oregon, USA. Moreover, factors such as evaporation, infiltration and runoff under different rainfall types were used for feature recognition to predict the Baishuihe landslide displacements between April 2007 and December 2008 (Liu et al. 2016). Martelloni et al. (2013) proposed the use of snow accumulation and melting as reference factors for an integrated model used in regional-scale landslide forecasting and early warning system. Finally, rainfall and water level are two significant factors always considered when analyzing mechanisms (Miao et al. 2020) or predicting displacement trends (Long et al. 2022) of landslides at the Three Gorges Reservoir in China.

As an essential landslide in the Three Gorges area, Baishuihe landslide has already been studied in many aspects, and various researches were already carried out to interpret its movements. In particular, many researchers studied its "step-like" displacement curve adopting a “decomposition” approach, according to which the real-time series is considered as the result of three overlapped displacement terms, one of each due to a different physical cause: the long-term related to the viscous trend, the periodic term due to the oscillations of the basin water level (Du et al. 2020; Du et al. 2012; Pei et al. 2021) and the residual term related to the climatic conditions (Jiang et al. 2021, Li et al. 2020; Liao et al. 2020; Liu et al. 2021; Wang et al. 2021; Zhang et al. 2020, Zhou et al. 2018; Zhu et al. 2018). After decomposition, different methods are applied to forecast the movements, such as Extreme Learning Machine (ELM) methods (Du et al. 2020; Huang et al. 2016; Lian et al. 2013; Liao et al. 2020), Binomial Regression with Back Propagation Neural Network (Du et al. 2012), Periodic Neural Network (PNN) (Liu et al. 2021), etc. Among them, the deep learning method was applied to Baishuihe landslide as well, like Long-Short Term Memory Network (LSTM) (Orland et al. 2020; Wang et al. 2021; Wang et al. 2021; Yang et al. 2019), Recurrent Neural Network (RNN) (Chen et al. 2013), Convolutional Neural Network (CNN) (Pei et al. 2021; Catani 2020), etc. However, all the studies mentioned above concentrated on evolution before 2018, when the stabilization project started. No evolution studies after stabilization works were performed yet, even if the landslide needs to be further studied to explore its displacement characteristics and regularity and evaluate the intervention effects. On the other hand, the mentioned decomposition approaches were generally

characterized by high time-consuming methods since they need to split the displacement data into two or three terms, analyze them separately making an individual prediction for each one and, finally, combining them up to provide the results.

In this paper, a new approach is proposed for analyzing the monitoring data recently collected at Baishuihe landslide, for exploring which factors and how they affect its current kinematic, and, finally, for optimizing the forecasting system for short and long-term warnings. The proposed approach maintains the original displacement time series and uses a time-frequency analysis. The displacement time series, together with those of rainfall, water level in the basin, and pore pressure measured in one piezometer, are elaborated with a multi-stage procedure coupling several tools for the signal analysis, specifically the Discrete Wavelet Transform (DWT), the Continuous Wavelet Transform (CWT) and the Convolutional Neural Network (CNN). The proposed method is an upgrade of the one proposed by Teza et al. (2022), previously successfully applied to the forecast of a landslide active in the North-East of Italy and implemented in the MATLAB toolbox named WADENOW, free supplied within an open-platform.

2. Methodology

In the initial version of WADENOW toolbox only two factors are related together: rainfall and landslide velocity. Here, in order to consider multi-factors to forecast landslide displacement trend, an upgraded version is developed to simultaneously process three parameters (velocity, rainfall, and difference between reservoir level and water table, which is proportional to pore pressure) and gain a more comprehensive application. In addition, in the new version the parameter combination is feasible, allowing to effectively evaluate and predict the combined impact of two or three factors on the target factor.

Figure 1 shows a flowchart which summarizes all the steps composing the improved version of WADENOW.

As depicted in Fig. 1, the procedure is subdivided into three main parts: data preprocessing, not existing in the previous WADENOW version; the scalogram generation and, finally, the CNN-based forecasting, whose inputs are the scalograms and output is the landslide motion prediction. In the tuning stage, the CNN training, validation and testing is carried out by using available data.

A new pre-processing step is added to obtain a filtered displacement rate time series. If the landslide displacement is measured with a fixed time step, for example by using GNSS stations, an interferometric radar or a robotized total station which acquire a series of retro-reflecting targets, it is possible to obtain the curve of displacement rate that can be in turn treated as a signal. If the landslide is very slow moving, i.e. the average velocity is between the 16 mm/y and 1.6 m/y (Cruden and Varnes 1996), where y indicates the non-SI unit “year”, the measuring errors induced by the monitoring system can generate velocity values that have no physically meaningful that have to be corrected by a denoising process. To solve this issue, the hourly displacement rate is computed and the result is denoised by using DWT to correct data without a physical meaning (e.g., negative values), leading to a reliable velocity value.

In the second part, the CWT is used to provide scalograms of physical factors affecting the phenomena. Scalogram images, which can be used as CNN inputs, are then obtained from scalograms. With respect to the first version in Teza et al (2022), the procedure is modified in order to allow the use of scalograms of two or three different monitoring quantities. The size of scalogram images is constrained by the CNN model used for transfer learning (Weiss et al. 2016).

A CNN learns to provide the forecasts by means of training, validation and testing. Since the aim is the tuning of a forecasting system, the input data are both scalogram images and the kinematic data which correspond to the same time steps of the forecasts in the operational stage. The data (input and output that should be reproduced) are subdivided into three subsets for training, validation and test respectively. In particular, training and validation are performed at the same stage. The training data are used to train the CNN, i.e., the model parameters are estimated by means of these data. The validation data are used in the same stage to evaluate the forecasting performance and prevent overtraining. Finally, in the testing stage the CNN performance is evaluated by computing and interpreting the confusion matrix. As such a stage is successfully completed, the CNN can be used to provide forecasts.

Obviously, it is necessary to train a specific CNN for each of the considered configurations (rainfall and velocity; pore pressure and velocity; rainfall, velocity and pore pressure), as depicted in Fig. 1.

In the following a brief description of the processing tools implemented in the methodology is provided.

2.1 Discrete Wavelet Transform (DWT)

In the Fourier transform, the base for the representation of a generic function consists of sinusoids having infinite duration; therefore, in the transform process the local information is lost. The wavelet transforms are based on wavelets with varying frequency and limited duration instead. In this way, a signal can be analyzed both in frequency and time. In particular, a DWT decomposes a given signal into a number of sets, where each set is a time series of coefficients describing the time evolution of the signal in the corresponding frequency band (Hosseinzadeh 2020).

In order to represent a signal by means of DWT, a mother wavelet and a corresponding scaling function are to be chosen. The wavelet coefficients obtained by projecting a signal onto scaled and time-translated versions of the scaling function are the approximation coefficients because they are related to different levels of approximation, whereas the wavelet coefficients obtained by projecting such a signal into scaled and time-translated versions of the mother wavelet are the detail coefficients because they encode the differences between two adjacent levels of approximation. The original time series can be reconstructed by means of inverse DWT (IDWT).

The DWT-based denoising is based on a fact that such a transform concentrates the signal features in a few large-magnitude wavelet coefficients. The wavelet coefficients which are small in value are typically noise and they can be removed (i.e., taken to zero) without affecting the signal information. After this treatment, the signal is reconstructed by means of IDWT. The DWT computation is performed by means

of filter banks, see e.g., Mallat (2008). Such an architecture has the advantage that the DWT can be implemented without the need to consider the explicit form of the scaling function and wavelets.

There are many wavelets that can be used for denoising, each of them with some advantages and disadvantages, e.g., Daubechies (Daubechies 1992), Biorthogonal (Cohen et al. 1992) and Coiflets (Burrus and Odegard 1997) Wavelets with similar properties may have different denoising performance; however, depending on the type of data, a specific wavelet could be more suitable (Cai and Harrington 1998). In this study, the Biorthogonal wavelet (Bior 3.1), which is characterized by biorthogonality, compactness and symmetry, was selected to denoise the kinematic data.

In the specific case, denoising is based on Bior 3.1, in which scaling constant equals to 3 and translating constant equals to 1. Moreover, wavelet decomposition level is carried out at the level 1 to ensure data fidelity, and the mode “periodic” is set to be run in signal decomposition and subsequent reconstruction. All these choices come from a trial-and-error approach based on real data.

2.2 Continuous Wavelet Transform (CWT)

The CWT of a signal y(t) is given by:

$$CWT\left(\alpha,\beta\right)=\frac{1}{\sqrt{\alpha}}\int_{-\infty}^{\infty}y\left(t\right)\psi^{*}\left(\frac{t-\beta}{\alpha}\right)dt$$

1

where $\psi\left(t\right)$ is the mother wavelet, i.e., is a zero-average oscillating function well localized both in time and frequency, $\alpha\neq0$ is the scaling constant, β is the translation in time and z^{*} is the complex conjugate of $z\in C$. As α and β change, the analysis of a non-stationary signal at multiple scales and different times can be carried out. The range of α and β are defined on the basis of the chosen mother wavelet and from the Nyquist frequency (half of sampling frequency). In the specific application, these ranges are automatically assigned by a WADENOW function.

Among the various possible CWT obtained by selecting different mother wavelet functions, the Morlet wavelet (Goupillaud et al. 1984) is particularly suitable for detecting and analyzing transient signals (Bello et al. 2005) and is often used mainly as a mother wavelet for CWT of geophysical time series, including climatological and meteorological data (Hochman et al. 2019). The complex Morlet wavelet with center frequency f_0 and time decay parameter σ_t^2 is an oscillation with a frequency f_0 tapered by a Gaussian window with variance σ_t^2, i.e.:

$$\psi\left(t\right)=\frac{1}{\sqrt{2\pi}\sigma_t}\exp\left(i2\pi f_0 t\right)\exp\left(-\frac{t^2}{2\sigma_t^2}\right)$$

2
;

these two parameters are such that (Cohen 2019):

$$\sigma_t = \frac{n}{2\pi f}$$

3

,

where *n* is the cycle count that governed the frequency domain energy spread and the time domain decay. In particular, as *n* grows, the CWT energy concentrates more at f_0, the wavelet decay in the time domain slows down, and the sinusoid oscillates more frequently. The selection of *n* and, consequently, σ_t^2, depends on the application. The result of CWT application is the scalogram, i.e., the CWT modulus, which represents the signal energy.

Scalogram images compatible with the subsequent CNN-based stage are generated by integrating two or three synchronous scalograms, one over the other, on a same image, depending on the number of input signals (velocity and rainfall, velocity and pore pressure, or also velocity, rainfall and pore pressure).

2.3 Convolutional Neural Network

The data provided by monitoring systems can be analyzed by means of artificial intelligence systems in order to obtain useful information regarding the studied phenomenon.

In general, a CNN consists of two parts:

(1) a convolutional base, aimed at generating some features from the input image and composed by a stack of convolutional and pooling layers;

(2) a classifier, aimed at classifying the image on the basis of the features detected by the convolutional base and usually composed of fully connected layers.

Here, a pre-trained CNN, i.e., the VGG19 model proposed by Simonyan and Zisserman (2015), is used for the recognition and classification of scalogram images after transfer learning. Transfer learning consists in replacing the original classifier with a new classifier that fits the new classification purposes by means of a specific training. In terms of the network architecture, the VGG19 CNN consists of 47 layers, among which there are 19 layers (16 convolutional layers and 3 fully connected layers). Additional layers like MaxPooling and dropout are also included (LeCun et al. 2015). Input images for VGG19 have size 224 x 224 pixels.

2.4 WADENOW toolbox

The WADENOW toolbox was upgraded in order to include DWT-based denoising, CWT-based scalogram generation and CNN-based scalogram classification for two or three input time series and to improve its power in movement-inducing factor evaluation and short-term forecasting.

Let t_c be a generic evaluation time, i.e., a time at which the monitoring data are to be analyzed and a forecast should be provided, expressed in days. As depicted in Fig. 2 the time span is set from $t_c - N_A$ to $t_c + N_B$, where N_A is the observation interval used for obtaining the forecasting and N_B the forecasting interval. In this application, N_A and N_B are set equal to 15 and 2 days, respectively. Figure 2(*a*) and (*b*) represent the schemes of the basic version of WADENOW with two parameters and the upgraded version with three parameters.

To implement the image classification, the velocity is used as a reference parameter for classifying the evolutional state of the landslide according to a typical displacement-time evolution of a creeping slope evolving towards failure (Fig. 3). The displacement-time curve could be divided in several portions: B is the threshold between an initial deformation stage AB and the constant deformation stage BC, while C is the threshold between the constant deformation stage BC and the acceleration stage CF preceding the collapse (Qiang et al. 2008).

Stage AB is always considered to be safe, while stage BC is a relatively stable state from which the landslide can have two evolutions: a subsequent increasing of the displacement rates (CF stage) up to reach the failure or a deceleration and a regression to the stable condition (AB stage). Most of the landslides in the reservoir are in stage BC. Within the stage CF, it is possible also to distinguish a span CD of low acceleration and a span DE of medium acceleration. When entering the EF span, i.e., the sliding acceleration stage, it is necessary to give the warning and evacuate the area.

As for the forecasting activity, seven landslide phases, from L_1 to L_7, are considered. These phases are obviously related to the above described landslide kinematic stages (Fig. 4). In particular, they are: L_1) phase of low speed; L_2) transition from low to medium speed, whose threshold is V_M; L_3) phase of medium speed; L_4) transition from medium to high speed, whose threshold is V_H; L_5) phase of high speed; L_6) deceleration from high to medium speed and L_7) deceleration from medium to low speed.

The output of CNN is the prediction of the landslide phase among L_1, …, L_7 on the basis of input data. In order to give an evaluation of the tool performance, it is necessary to compare the prediction with the reality by means of a confusion matrix. This is a matrix with two dimensions, one is indexed by the actual event, and the other is indexed by the event that the classifier predicts with the same input data.

Figure 5 shows the confusion matrix for a multi-event classification task, with the events A_1, A_2, to A_n. In the confusion matrix, N_{ij} represents the number of samples actually belonging to event A_i but classified as event A_j (Deng et al. 2016).

To quantify the reliability, two indexes are chosen in this paper:

1) Accuracy defined as the proportion between the correct predictions and the totality:

$$Accuracy = \frac{\sum_{i=1}^{n} N_{ii}}{\sum_{i=1}^{n}\sum_{j=1}^{n} N_{ij}}$$

4

2) Precision is a measure providing how many times a specific event is correctly predicted, according with the definition:

$$Precision = \frac{N_{ii}}{\sum_{k=1}^{n} N_{ki}}$$

5

3. Case study: Baishuihe Landslide

3.1 Landslide general features

Baishuihe landslide is a large-scale deep-seated landslide located in the administrative area of Zigui County, Hubei Province (31° 01' 34" N, 110° 32' 09" E), 56 km uphill of the Three Gorges Dam along the Yangtze River (Fig. 6).

The elevation of the summit point is 297 m a.s.l. with the main crack as the rear boundary (Fig. 7). The lower point is at an elevation of about 120–130 m a.s.l. which is always below the water level of the Yangtze River reservoir (about 145 m a.s.l.). The landslide spreads 500 m long from North to South and 430 m wide from East to West, covering an area of 215,000 m^2 with a shape of an “irregular circle” (Li et al. 2009). Its average thickness is about 30 m (Fig. 8) and its volume is 6.45×10^6 m^3. The main sliding direction is from SSW to NNE, along the slope dip direction and toward the Yangtze River.

The body of the landslide is constituted by a chaotic loose material within which a uniform layering is not recognizable. There is not a continuous unique base at the contact with the lower rock and the thickness of the sliding mass varies between 7.5 and 37.7 m (Fig. 8). The zone where the sliding movements are concentrated is mainly composed of silty clay containing gravel or breccia fragments with a thickness varies from 0.2 to 1.3 m with an average value of 0.7 m. The stable bedrock is mainly composed of the Jurassic Xiangxi Formation (J_{1x}), a stratified siltstone-mudstone, with a dip direction of 15°N and a mean dip angle of 36°.

3.2 Evolutionary Process

According to the displacement data and the macroscopic deformation characteristics of Baishuihe landslide, it was divided into three parts (Fig. 6(*c*)): two warning areas (W1 and W2), showing the major intensity of deformation, and one non-warning area (N), where only low intensity deformation was observed. Deformation occurs mainly during the flood season, generating the gradual formation of many

cracks, some of which did not expand until landslide failure while others were eliminated during the stabilization project.

3.3 Monitoring systems and stabilization works

Figure 7 shows the monitoring system originally implemented after the first macroscopic deformations, since June 2003. A total of 11 manual monitoring stations were set up: 5 in N area (ZG91, ZG92, ZG94, ZG119, ZG120) and 6 in W1 and W2 areas (ZG93, ZG118, XD-01, XD-02, XD-03, XD-04). Since the water level in Three Gorges Reservoir reached 175m in 2008, XD-02, XD-03 and XD-04 are submerged by the water during every flood season.

In October 2018, to prevent the landslide from other displacements and endanger the safety of shipping in the Yangtze River, the landslide was subjected to some stabilization interventions. The project includes (Fig. 10): stabilization of the slope toe with a backfill; reduction of rainwater infiltration with four large drainage trenches installed along the slope from the top to the toe; drainage of surficial water in the left side of the slope with a short drainage culvert; protection of the relatively steep areas with a cover turf; excavation of a large volume above the steep area to reduce the weight of the upper slope, prevent rockfalls and improve the overall stability; realization of a retaining wall on the rear part of the excavated area to protect the riverside road crossing from one side to the other the landslide area. In the two years after the work the landslide displacement trend slowed down significantly, as shown in Fig. 12.

In addition to the works, a new monitoring system (Fig. 11) was installed for checking the mitigation effect gave by interventions and the subsequent slope kinematic. A total number of 10 GNSS stations, including 4 stations (DB4, DB5, DB7 and DB8) with automatic recording every hour and 6 (DB1, DB2, DB3, DB6, DB9 and DB10) with manual registration, are devoted for the surficial displacement monitoring. To complete the system there are 4 groundwater monitoring stations, SW1, SW2, SW3, and SW4, reaching depths of 23 m, 24 m, 23.5 m, and 31 m, respectively.

3.4 Analysis of data after stabilization works

In Fig. 12 the displacements accumulated with time at the stations ZG93, ZG118 and XD-01, installed in 2003, are compared with the reservoir water level and the monthly rain. It is evident as consequently to the rise of the maximum water level in the reservoir, from about 140 m to 145 m in 2003 and then to 155 m in 2006, a “step-like” deformation appeared with the majority of annual displacements occurring in the rainy season. A relatively large displacement increment appeared in 2015, probably due to a cruise capsizing occurred in the Yangtze River which led to the abnormal regularity of reservoir water level (Yang et al. 2017). Next, the “step-like” deformation started to slow down from the beginning of 2019 during the stabilization work realization and the same displacement trend is maintained after their completion.

Figure 13 shows a detail of the previous plot in the period from October 2018, when the stabilization started, to the end of 2021. In addition to the reservoir water level and the daily rain, the displacement

observed at the new station DB5 and the groundwater level in SW1 are also reported. When zooming the displacement graph, the “step-like” trend, even if less evident as in the past years, is also present.

Figure 13 clearly shows that the groundwater table (GWT) in SW1 is strongly related to the reservoir water level (RWL) and to the rain. In fact, when in the winter season the RWL is high, i.e., over 169 m, the GWT in SW1 is at the same level. On the contrary when the reservoir is drained and its water level goes below 169m, the GWT in SW1 remains high and the difference ΔW between the two levels increases reaching maximum value to 32.6 m. It is also easy to note that when a heavy rainfall occurs a rise to 10 m of GWT in SW1 can be observed only if the RWL is lower than 169 m. The “step-like” displacement seems occur precisely at this stage: on the contrary, if a rainy event occurs when the RWL is high, no oscillation of GWT in SW1 appears.

In order to evidence this behavior, three events of deformation with different conditions of rainfall, RWL and GWT in the piezometer are selected in the period 2020–2021 and the impacts of rainfall and RWL are qualitatively analyzed. According to Fig. 14(*a*), during August every year, the RWL fluctuates and heavy rainfall rarely happens in this period. The velocity oscillates around the zero value, showing also negative values due to the difficulty of accurately calculating this quantity. In fact, the velocity is obtained as the difference between the measured values of accumulated displacement into subsequent instants: if the landslide moves very slowly, like it happens after the stabilization project, a small measuring error in the displacement can give a negative difference that, of course, has no physical meaning because a landslide does not come back. From this example, it cannot be concluded that the RWL and GWT have no influence on velocity because it seems that its variation has no effect.

A second typical situation, reported in Fig. 14(*b*), occurs after the rainy season in mid-November. The reservoir water keeps to the maximum level and GWT does the same. In general, apart from some oscillations, the landslide in this period can be considered in a stable state, despite some intense rainfall episodes. Similar with RWL and GWT, the rainfall still cannot be considered a factor surely affecting the displacement velocity.

Finally, in Fig. 14(*c*) it is reported what occurred from the beginning to the end of July 2021. In this rainy period, while the water level in the reservoir is maintained around 145m, the heavy rainfall induces a temporary increase of the water table in the piezometer with respect to the level in the reservoir. At once, it is observed a significant increase in the displacement velocity, which has consistency with both rainfall and GWT.

Due to the uncertainty of the cases above, it is necessary to quantify how much these factors affect the deformation after intervention. As it is well-known, hydrodynamic pressure is one of the main elements affecting landslide kinematic mechanisms. Therefore, the difference of RWL and GWT, here defined as ΔW, was used in the model as an indirect measure of the hydrodynamic pressure acting inside the landslide body. Consequently, in the following, the factors used in this study are ΔW, rainfall and displacement velocity.

4. Calculation and results

In order to have a more significant series of velocity for studying the kinematic behavior of Baishuihe after stabilization, only the data series of the station DB5 from the 1st November 2019 to the 31st December 2021 is used. After application of the previously described denoising procedure with Bior 3.1 Wavelet, the database composed by approximately 19750 hourly data is subdivided in three parts: about 70% of it is used for training the CNN model, 15% for the validation and then 15% for the prediction, and finally evaluating its reliability is necessary.

Regarding the velocity thresholds V_H and V_M, identifying the points B and C (Fig. 3), these values are "landslide specific". Based on the data from automatic GPS monitoring stations since 2003 to 2018, in every rainy season, Baishuihe entered in DE stage, even sometimes in EF stage. However, after stabilization work, the velocity is strongly reduced and to better classify the velocity state of Baishuihe it is convenient to adopt two velocity thresholds within the range CD of the initial acceleration, for instance, points G and H. For this reason, also in this case, like in the original application of WADENOW, it was adopted velocity thresholds V_H and V_M equal to 13.7 mm/d and 9.5 mm/d, respectively.

According to this choice, the time series of rainfall, ΔW and velocity are classified in the groups L_1 – L_7 and the relative scalograms are obtained. Figure 15 and Fig. 16 show some typical scalograms for the various L_1 – L_7 groups obtained with CWT in analysis considering 2 or 3 factors at once.

In the first case (2 factors analysis), two configurations are considered: one considering rainfall (R) and velocity (V) scalograms together (Fig. 15(*a*)), the other considering rainfall R and ΔW scalograms (Fig. 15(*b*)).

On the other side, Fig. 16 shows the scalograms of analysis with all the factors (R–ΔW–V) together.

5. Evaluation and comparison

Tens of thousands of images were used to form the scalogram dataset to be transferred into CNN. After training and validation of CNN, performed using the 70% and 15% of the entire database, respectively, the confusion matrix is obtained on the basis of the last portion of database (15% of all). Figure 17 shows the confusion matrices of 2-factors configurations (i.e., R vs V and ΔW vs V, respectively), while Fig. 18 shows the confusion matrix of 3-factors configuration (i.e., R + ΔW vs V).

Then accuracy and precision were used to compare and analyze as Fig. 19 shows.

The values of accuracy show that the overall accuracy of prediction obtained on the basis of a single factor (rainfall or difference of levels) is very good, e.g., equal to 94.2% with both the factors, while with their combination the accuracy is a little bit smaller (94.1%) but still satisfying.

Looking at the precision, it is not possible to arrive at a unique judgement, because this parameter presents different values for each phase. The L_1 phase always happens when the reservoir water level

RWL starts to draw down in March every year. With the RWL drawing down, the hydrodynamic pressure, considered by ΔW in the analysis, generates. However, at the same moment, the rainfall occurs and the landslide deformation starts to develop. For this reason, the precision of CNN based on R only is high (96.7%) but it increases more when adding the factor is ΔW reaching to 98.7%.

From April to June in every year, the RWL is drawing down and hydrodynamic pressure gradually increases. This condition generally happens in the groups L_2, L_3 and L_4, for which it is evident that ΔW plays a dominant role in deformation speeding up and the precision of the ΔW scalogram is the highest among the three possible combinations of factors (98.8%, 92.9% and 93.2%, respectively).

The “step-like” phase appears exactly immediately after this period and is contained in the L_5, when the displacement rate reaches the highest values. This condition is no longer determined by a single factor but by the combination of R and ΔW: the prediction precision of the double scalograms reaches in absolute the highest value among all the cases (99.1%).

If heavy or continuous rainfall occurs when the RWL is at its minimum value, the velocity will be pushed to within the high-speed deformation range (L_5 phase). It is a common phenomenon in the rainy season in June, July and August. For this reason, also rainfall has a fundamental rule, as depicted by the CNN based only on R for phase L_5.

In phase L_6 rainfall is dominant with a CNN precision (96.6%) higher respect of precision of CNN based only on ΔW or the combination of rainfall and ΔW. In this state, the landslide begins to decelerate from high to medium speed and this generally happens in September, when RWL is risen and the hydrodynamic pressure reduces progressively.

Finally, phase L_7 is when RWL reaches the maximum value, e.g., 175 m. A very high RWL stabilizes the landslide and in the meanwhile a small rainfall can cause low-speed deformation. In this case, the result shows that the combined factors, whose CNN precision is 96.8%, are more efficient for predicting L_7.

6. Discussion and conclusion

This study upgraded a DWT-CWT-CNN-based forecasting procedure. The upgrade is based on displacement rate evaluating the influence magnitude of various factors in a specific kinematic state and predicting the future displacement change trend. Finally, the upgrade version is here applied to the case of Baishuihe landslide in Three Gorges Reservoir in China.

At first, Baishuihe is a well-known landslide that many researchers have already extensively studied because, in the years, it has developed very large deformation. The regular “step-like” displacement evolution displayed in the period 2003–2018 was clearly caused by the periodic fluctuation of the reservoir water level, but after the stabilization works carried out in 2018–2019 the deformation evolution underwent a complete change. The “step-like” behavior becomes less evident, especially starting from the second year, and the effect of rainfall seems to be predominant. According to the velocity classification,

at present the velocities are in the ranges of initial deformation, constant deformation and initial acceleration stages. It can be summarized that after interventions Baishuihe landslide is quasi-entirely stabilized.

Secondly, even if the risk is surely mitigated and the laws of deformation in years before stabilization are no longer applicable to the current Baishuihe landslide, a landslide status evaluation coupled with an early warning still remains a very effective and timely strategy for the correct management of the area. To this purpose and to better evidence the effects of various factors, the deep learning method here proposed considers landslide monitoring data such as rainfall, reservoir water level, groundwater table and specific velocity, the last one evaluated on the base of surficial displacement time series. On the basis of these data the procedure generates scalograms, which are variously combined to form the images sent to the deep learning procedure. The selection of these parameters is conditioned by the existing database in this case study, but, if the method have to applied for the analysis of other landslides, they can be changed according to the available dataset: consequently, the surficial velocity could be substituted with the rate of deep displacement variation obtained on the base of data acquired by an inclinometer or an extensometer, or, it may be that other parameters, for instance the temperature or the snow area covering, could have larger influence.

Finally, the here developed procedure reveals the accuracy and precision of Baishuihe landslide forecast under different factors: rainfall, hydrodynamic pressure, displacement rate and their combination. There is not a unique result, because depending on the landslide status a better prediction can be obtained or on the base of only one single factor or considering the influence of different factors. Rainfall mainly affects the phases L_1 (activation of slow mobility) and L_6 (deceleration), whereas hydrodynamic pressure plays a dominant role in more significantly accelerating the deformation (L_2, L_3, and L_4 phases), In addition, in the high-speed phase L_5, the resulting velocity is affected by the combination of rainfall and hydrodynamic pressure: although the prediction precision using a single factor is high (97.2% for rainfall and 97.9% for ΔW), the coupling of these factors pushes up the precision of prediction even more to 99.1%. In conclusion, it is proved that both rainfall and hydrodynamic pressure play a dominant role in the trigger of Baishuihe landslide deformation, but their combination could push the displacement rate even higher.

It is important to emphasize that having more than one CNN makes it possible to obtain forecasts even if one of the monitoring systems is temporarily unable to provide data. For example, if it were not possible to have data about pore pressure, it would still be possible to obtain predictions using only velocity and rainfall.

The computation time required for CNN training/validation/test is around 45 min for each of the two inputs and 55min for the three inputs configuration respectively, with a PC with Intel i9-10900 CPU @ 3.7GHz (GPU accelerated), 16.0 GB RAM. This means that the proposed approach is completely compatible with the typical currently available computation resources. Moreover, as the CNNs are trained, the complete forecast computation, including data pre-filtering, can be carried out instantly after the data

receiving. Since the time for completing data acquisition and transmission is less on the order of few minutes maximum, this means that forecasts are promptly available.

The fact that the reference CNN used for transfer learning allows 224x224 input images limits the number of possible scalograms that can be represented in the same image. With three scalograms it is still possible to maintain adequate frequency details. Note that this implies limitations on the choice of N_A. Future CNN models could be not affected by these size limits.

Referring to the application, the program demonstrated to be very sensitive to the velocity change in the reservoir landslide cases, especially when the RWL changes and groundwater in the slope cannot follow it in time: this produce a dynamic water pressure which can be considered trough the parameter DW. In addition, short-term heavy rainfall can also be obviously identified. It always causes pore pressure suddenly rising, then breaks the equilibrium. Therefore, on the geological aspect, the program is more inclined to be applied to slopes constituted by low permeability soils or weathered rocks.

This study is based on an upgraded version of WADENOW, a short-term prediction system of landslide velocity proposed as a significant reference value for monitoring and early warning. At the same time, it can also quantitatively determine the influence of triggering factors and implement a forecast. To sum up, from the result, it turns out that the procedure is valid for landslide prediction and the upgraded version is flexible to be applied on multi-factors affecting landslides and provide support for landslide early warning. In areas where landslides are concentrated, it can conveniently evaluate landslide status, distinguish factors and predict future kinematic evolution. This is especially important in the Three Gorges Reservoir area where, since the reservoir was impounded to 175m in 2009, more than 5,000 landslides have been found and hundreds of landslides are being well monitored. Here this method can provide reference values for regional landslide management.

Declarations

Funding

The authors declare that no funds, grants, or other support were received during the preparation of this manuscript

Competing Interests

The authors declare that they have no known competing financial interests or personal relationships that could have appeared to influence the work reported in this paper.

Author Contribution

All authors contributed to the study conception and design. Material preparation, data collection and analysis were performed by Yuting Liu, Lorenzo Nava and Simonetta Cola. Basic program was coded by Giordano Teza and the program used in this article was upgraded by Yuting Liu. The first draft of the

manuscript was written by Yuting Liu and all authors commented on previous versions of the manuscript. All authors read and approved the final manuscript.

References

1. Ahmad J, Farman H, Jan Z (2019) Deep Learning Methods and Applications. In: Deep Learning: Convergence to Big Data Analytics. SpringerBriefs in Computer Science. Springer, Singapore, pp 31-42. https://doi.org/10.1007/978-981-13-3459-7_3
2. Bello J P, Daudet L, Abdallah S, Duxbury C, Davies M, Sandler M B (2005) A tutorial on onset detection in music signals. IEEE Transactions on Speech and Audio Processing. 13**:** 1035-1047. https://ieeexplore.ieee.org/document/1495485
3. Burrus C, Odegard J E (1997) Generalized coiflet systems. Proceedings of 13th International Conference on Digital Signal Processing. 97, 321-324. https://ieeexplore.ieee.org/abstract/document/628083
4. Cai C, Harrington P d B (1998) Different Discrete Wavelet Transforms Applied to Denoising Analytical Data. Journal of Chemical Information and Computer Science. 38**:** 1161-1170. https://pubs.acs.org/doi/full/10.1021/ci980210j
5. Catani F (2020) Landslide detection by deep learning of non-nadiral and crowdsourced optical images. Landslides. 18: 1025-1044. https://doi.org/10.1007/s10346-020-01513-4
6. Chen H, Zeng Z, Tang H (2015) Landslide Deformation Prediction Based on Recurrent Neural Network. Neural Processing Letters. 41**:** 169-178. https://doi.org/10.1007/s11063-013-9318-5
7. Cohen A, Daubechies I, Feauveau J-C (1992) Biorthogonal Bases of Compactly Supported Wavelets. Communications on pure and applied mathematics. 45**:** 485-560. https://doi.org/10.1002/cpa.3160450502
8. Cohen M X (2019) A better way to define and describe Morlet wavelets for time-frequency analysis. Neuroimage. 199**:** 81-86. https://doi.org/10.1016/j.neuroimage.2019.05.048
9. Cruden D M, Varnes D J (1996) Landslide types and processes. In: Landslides: Investigation and Mitigation. R. L. Schuster. Washington, DC**,** pp 36-75.
10. Daubechies I (1992) Ten Lectures on Wavelets. Society for industrial and applied mathematics. Philadelphia, Pennsylvani.
11. Deng X, Liu Q, Deng Y, Mahadevan S (2016) An improved method to construct basic probability assignment based on the confusion matrix for classification problem. Information Sciences. 340-341**:** 250-261. https://doi.org/10.1016/j.ins.2016.01.033
12. Du H, Song D, Chen Z, Shu H, Guo Z (2020) Prediction model oriented for landslide displacement with step-like curve by applying ensemble empirical mode decomposition and the PSO-ELM method. Journal of Cleaner Production. 270, 122248. https://doi.org/10.1016/j.jclepro.2020.122248
13. Du J, Yin K, Lacasse S (2012) Displacement prediction in colluvial landslides, Three Gorges Reservoir, China. Landslides. 10**:** 203-218. https://doi.org/10.1007/s10346-012-0326-8

14. Goupillaud P, Grossmann A, Morlet G (1984) Cycle-octave and related transforms in seismic signal analysis. 23**:** 85-102. https://doi.org/10.1016/0016-7142(84)90025-5
15. Hosseinzadeh M (2020) Robust control applications in biomedical engineering: Control of depth of hypnosis. In: Ahmad T A (ed) Control Applications for Biomedical Engineering Systems**,** Academic Press, pp 89-125. https://doi.org/10.1016/B978-0-12-817461-6.00004-4
16. Huang F, Yin K, Zhang G, Gui L, Yang B, Liu L (2016) Landslide displacement prediction using discrete wavelet transform and extreme learning machine based on chaos theory. Environmental Earth Sciences. 75, 1376. https://doi.org/10.1007/s12665-016-6133-0
17. Jiang Y, Xu Q, Lu Z, Luo H, Liao L, Dong X (2021) Modelling and predicting landslide displacements and uncertainties by multiple machine-learning algorithms: application to Baishuihe landslide in Three Gorges Reservoir, China. Geomatics, Natural Hazards and Risk. 12**:** 741-762. https://doi.org/10.1080/19475705.2021.1891145
18. LeCun Y, Bengio Y, Hinton G (2015) Deep learning. Nature. 521: 436-44. https://doi.org/10.1038/nature14539
19. Li D, Yin K, Leo C (2009) Analysis of Baishuihe landslide influenced by the effects of reservoir water and rainfall. Environmental Earth Sciences. 60**:** 677-687. https://doi.org/10.1007/s12665-009-0206-2
20. Li L, Wu Y, Miao F, Xue Y, Huang Y (2020) A hybrid interval displacement forecasting model for reservoir colluvial landslides with step-like deformation characteristics considering dynamic switching of deformation states. Stochastic Environmental Research and Risk Assessment. 35**:** 1089-1112. https://doi.org/10.1007/s00477-020-01914-w
21. Lian, C., Zeng, Z., Yao, W. et al (2013) Displacement prediction model of landslide based on a modified ensemble empirical mode decomposition and extreme learning machine. Natural Hazards 66: 759-771. https://doi.org/10.1007/s11069-012-0517-6
22. Liao K, Wu Y, Miao F, Li L, Xue Y (2020) Using a kernel extreme learning machine with grey wolf optimization to predict the displacement of step-like landslide. Bulletin of Engineering Geology and the Environment. 79**:** 673-685. https://doi.org/10.1007/s10064-019-01598-9
23. Liu Q, Lu G, Dong J (2021) Prediction of landslide displacement with step-like curve using variational mode decomposition and periodic neural network. Bulletin of Engineering Geology and the Environment. 80**:** 3783-3799. https://doi.org/10.1007/s10064-021-02136-2
24. Liu Y, Liu D, Qin Z, Liu F, Liu L (2016) Rainfall data feature extraction and its verification in displacement prediction of Baishuihe landslide in China. Bulletin of Engineering Geology and the Environment. 75**:** 897-907. https://doi.org/10.1007/s10064-015-0847-1
25. Long J, Li C, Liu Y, Feng P, Zuo Q (2022) A multi-feature fusion transfer learning method for displacement prediction of rainfall reservoir-induced landslide with step-like deformation characteristics. Engineering Geology. 297, 106494. https://doi.org/10.1016/j.enggeo.2021.106494.
26. Mallat S (2008) A Wavelet Tour of Signal Processing. San Diego, California.

27. Martelloni G, Segoni S, Lagomarsino D, Fanti R, Catani F (2013) Snow accumulation/melting model (SAMM) for integrated use in regional scale landslide early warning systems. Hydrology and Earth System Sciences. 17: 1229-1240. https://doi.org/10.5194/hess-17-1229-2013
28. Miao F, Wu Y, Li L, Liao K, Xue Y (2020) Triggering factors and threshold analysis of baishuihe landslide based on the data mining methods. Natural Hazards. 105: 2677-2696. https://doi.org/10.1007/s11069-020-04419-5
29. Miao F, Wu Y, Xie Y, Yu F, Peng L (2016) Research on progressive failure process of Baishuihe landslide based on Monte Carlo model. Stochastic Environmental Research and Risk Assessment. 31: 1683-1696. https://doi.org/10.1007/s00477-016-1224-8
30. Orland E, Roering J J, Thomas M A, Mirus B B (2020) Deep Learning as a Tool to Forecast Hydrologic Response for Landslide-Prone Hillslopes. Geophysical Research Letters. 47, 16. https://doi.org/10.1029/2020GL088731
31. Pei H, Meng F, Zhu H (2021) Landslide displacement prediction based on a novel hybrid model and convolutional neural network considering time-varying factors. Bulletin of Engineering Geology and the Environment. 80: 7403-7422. https://doi.org/10.1007/s10064-021-02424-x
32. Qiang X, Minggao T, Kaixiang X, Xuebin H (2008) Research on space-time evolution laws and early warning-prediction of landslides. Chinese Journal of Rock Mechanics and Engineering. 27: 1104-1112. (In Chinese)
33. Song K, Wang F, Yi Q, Lu S (2018) Landslide deformation behavior influenced by water level fluctuations of the Three Gorges Reservoir (China). Engineering Geology. 247: 58-68. https://doi.org/10.1016/j.enggeo.2018.10.020
34. Tehrani F S, Calvello M, Liu Z, Zhang L, Lacasse S (2022) Machine learning and landslide studies: recent advances and applications. Natural Hazards. 114, 1197–1245. https://doi.org/10.1007/s11069-022-05423-7
35. Teza G, Cola S, Brezzi L, Galgaro A (2022) Wadenow: A Matlab Toolbox for Early Forecasting of the Velocity Trend of a Rainfall-Triggered Landslide by Means of Continuous Wavelet Transform and Deep Learning. Geosciences. 12, 205. https://doi.org/10.3390/geosciences12050205
36. Wang H, Long G, Liao J, Xu Y, Lv Y (2021) A new hybrid method for establishing point forecasting, interval forecasting, and probabilistic forecasting of landslide displacement. Natural Hazards. 111: 1479-1505. https://doi.org/10.1007/s11069-021-05104-x
37. Wang J, Nie G, Gao S, Wu S, Li H, Ren X (2021) Landslide Deformation Prediction Based on a GNSS Time Series Analysis and Recurrent Neural Network Model. Remote Sensing. 13, 1055. https://doi.org/10.3390/rs13061055
38. Wang Y, Tang H, Huang J, Wen T, Ma J, Zhang J (2022) A comparative study of different machine learning methods for reservoir landslide displacement prediction. Engineering Geology. 298, 106544. https://doi.org/10.1016/j.enggeo.2022.106544
39. Weiss K, Khoshgoftaar T M, Wang D (2016) A survey of transfer learning. Journal of Big Data. 3, 9. https://doi.org/10.1186/s40537-016-0043-6

40. Xu D, Peng L, Liu S, Wang X (2018) Influences of Risk Perception and Sense of Place on Landslide Disaster Preparedness in Southwestern China. International Journal of Disaster Risk Science. 9**:** 167-180. https://doi.org/10.1007/s13753-018-0170-0
41. Yang B, Yin K, Lacasse S, Liu Z (2019) Time series analysis and long short-term memory neural network to predict landslide displacement. Landslides. 16: 677-694. https://doi.org/10.1007/s10346-018-01127-x
42. Zhang J, Tang H, Wen T, Ma J, Tan Q, Xia D, Liu X, Zhang Y (2020) A Hybrid Landslide Displacement Prediction Method Based on CEEMD and DTW-ACO-SVR-Cases Studied in the Three Gorges Reservoir Area. Sensors (Basel). 20, 4287. https://doi.org/10.3390/s20154287
43. Zhou C, Yin K, Cao Y, Intrieri E, Ahmed B, Catani F (2018) Displacement prediction of step-like landslide by applying a novel kernel extreme learning machine method. Landslides. 15**:** 2211-2225. https://doi.org/10.1007/s10346-018-1022-0
44. Zhu X, Xu Q, Tang M, Li H, Liu F (2018) A hybrid machine learning and computing model for forecasting displacement of multifactor-induced landslides. Neural Computing and Applications. 30**:** 3825-3835. https://doi.org/10.1007/s00521-017-2968-x

Figures

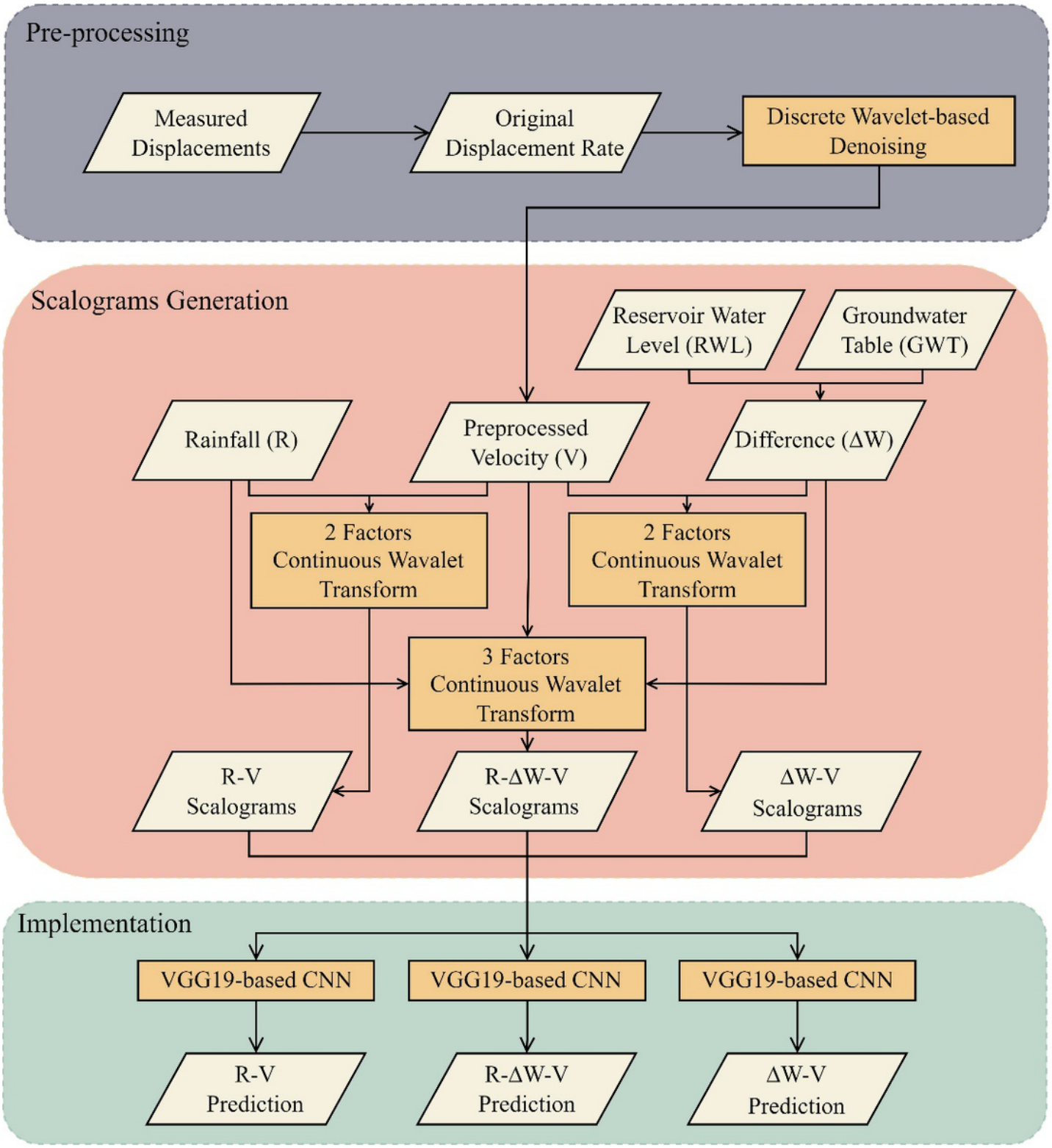

Figure 1

Flowchart of the new multi-stage analysis method

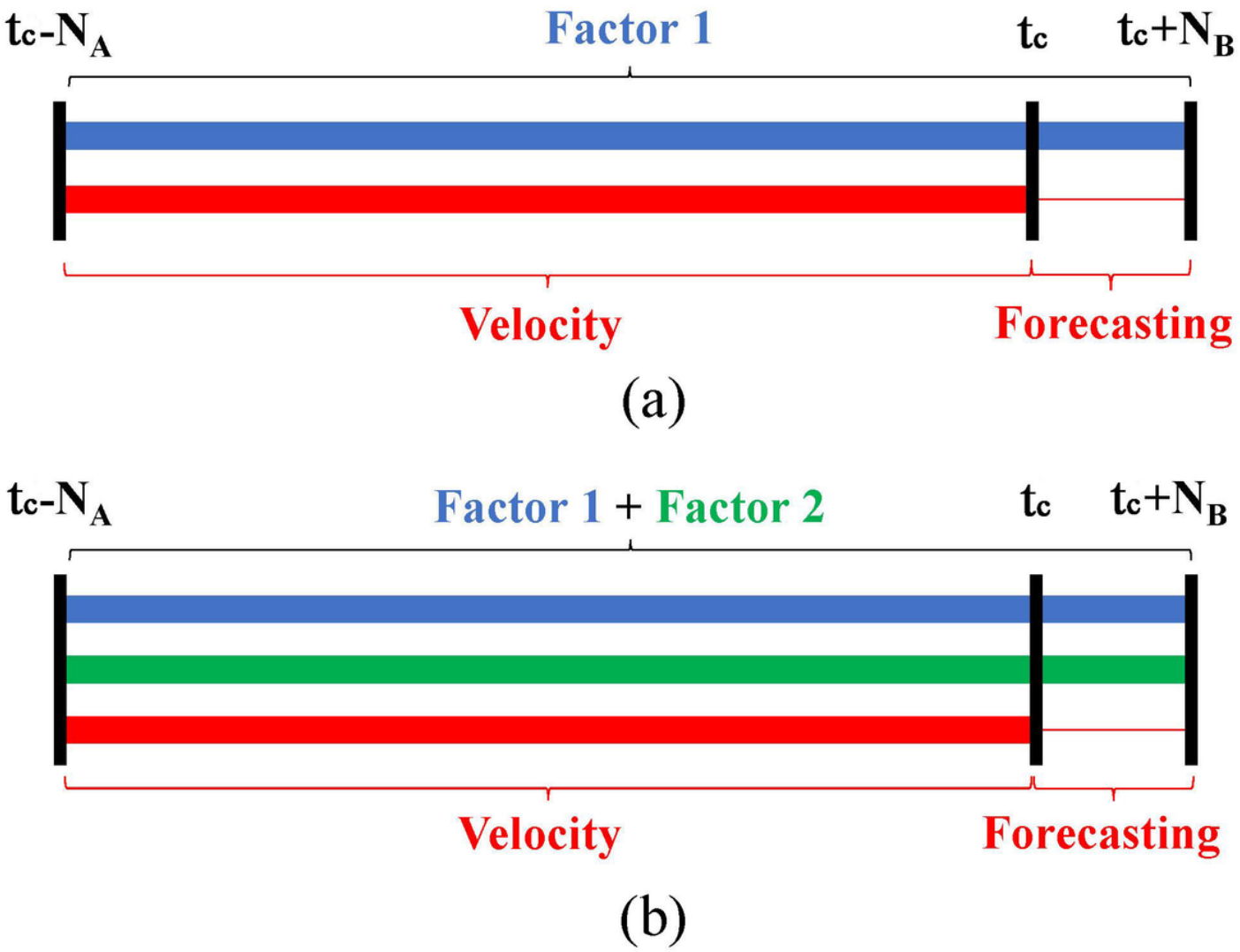

Figure 2

Schematic configurations of forecasting model in configuration with one or two factors related to the velocity

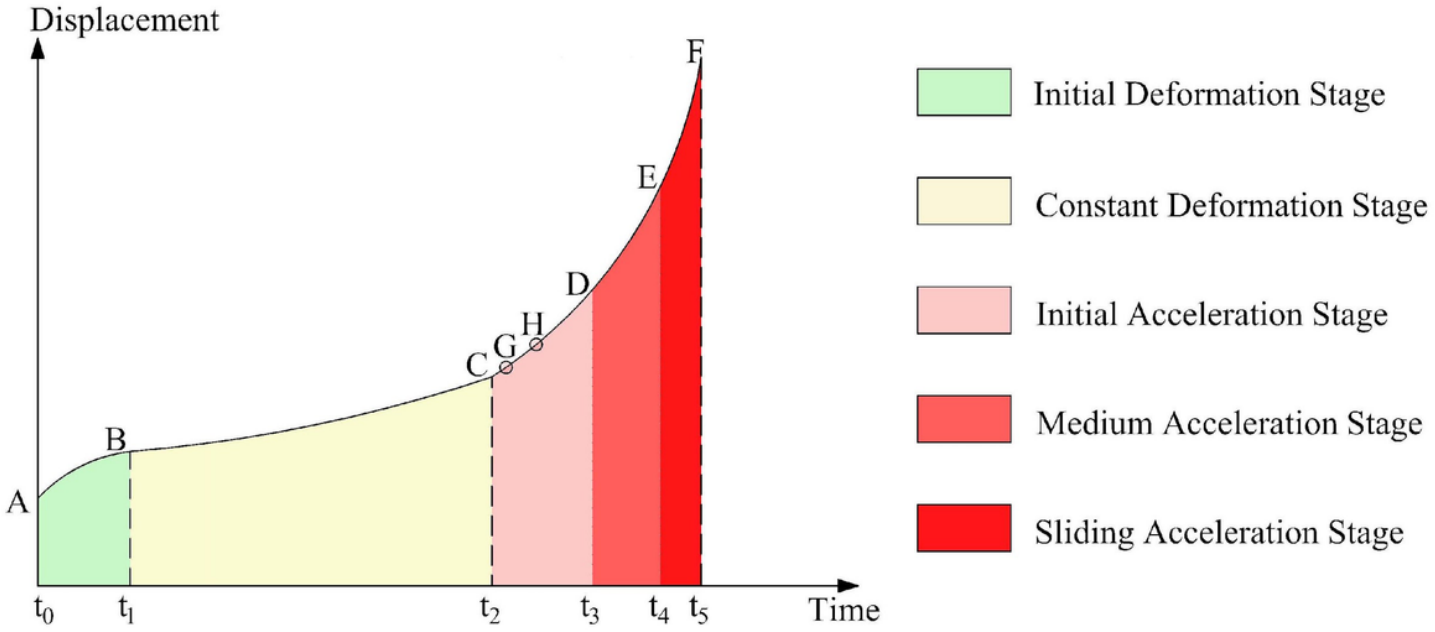

Figure 3

Sketch of various deformation phases of a slope evolving to failure (Qiang et al. 2008)

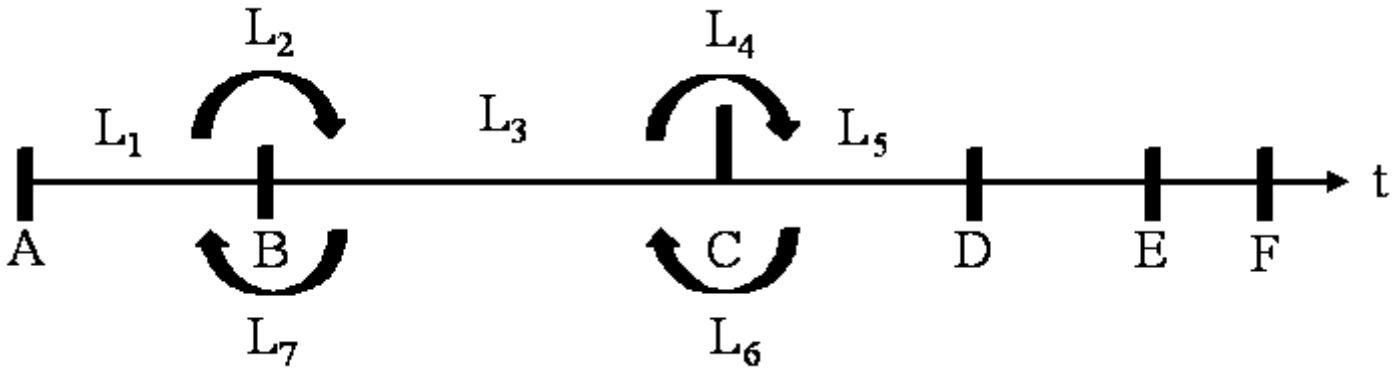

Figure 4

Scheme of seven classified events

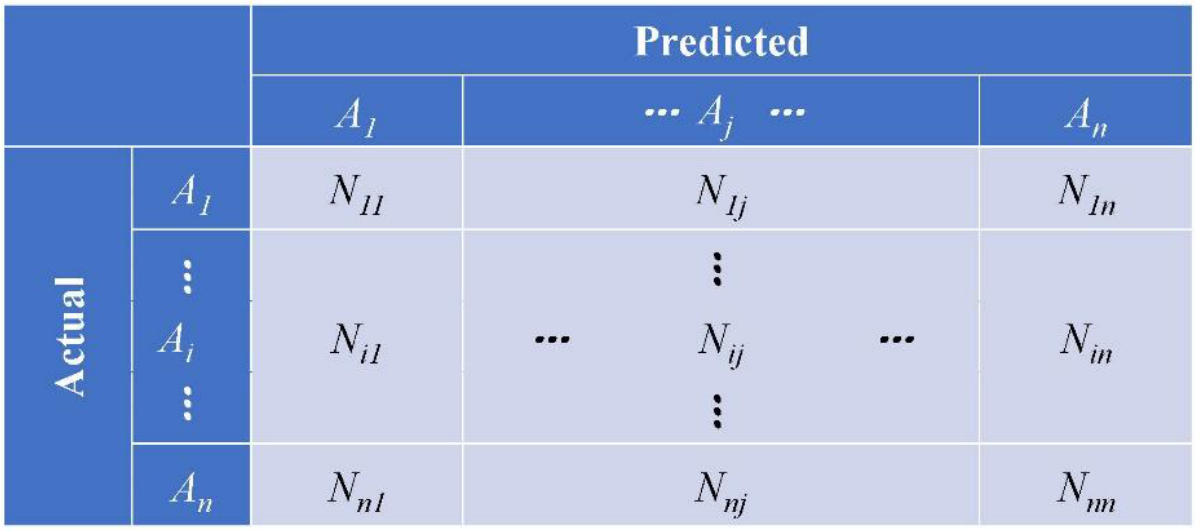

Figure 5

Confusion Matrix

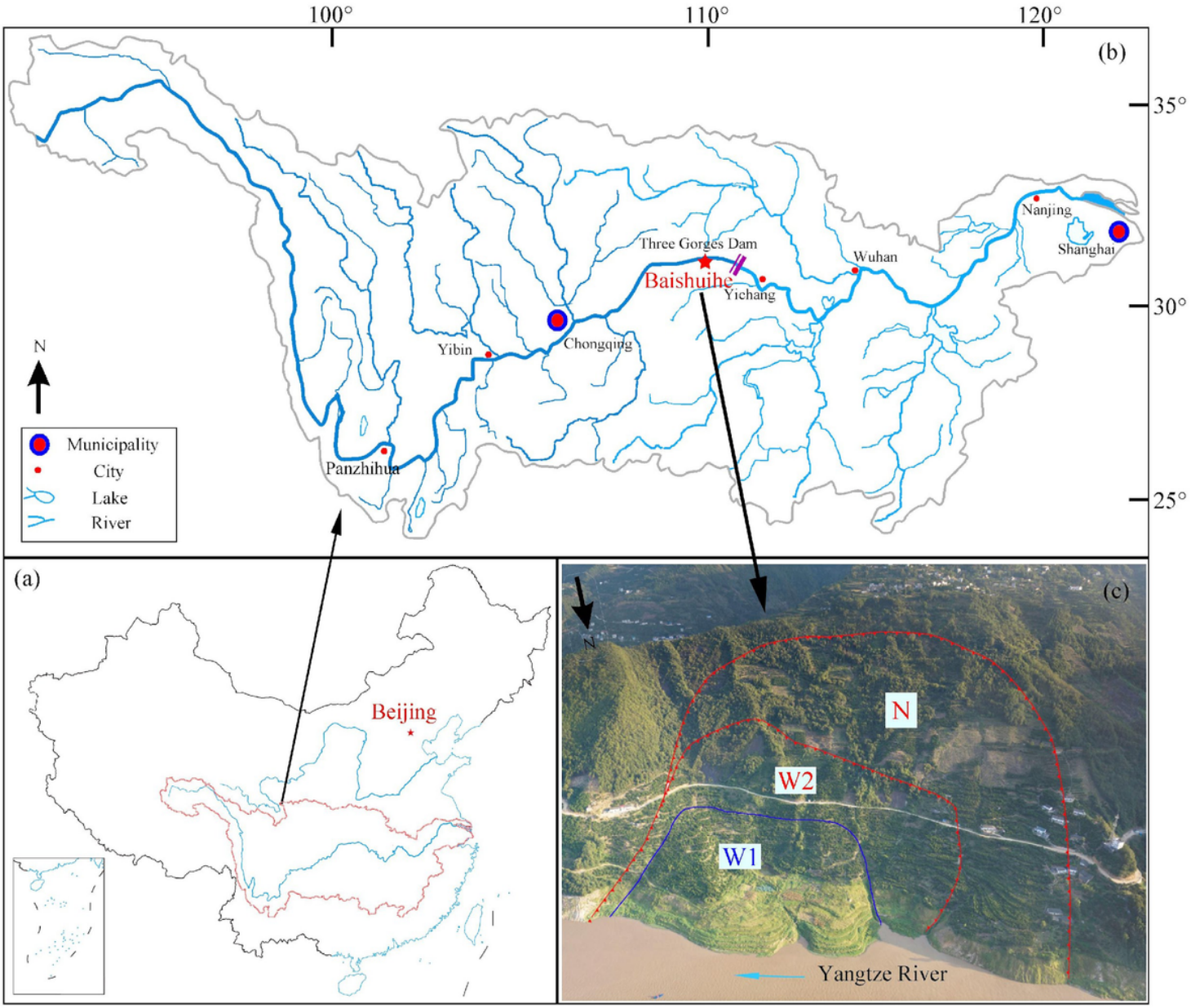

Figure 6

Location of Baishuihe landslide in Three Gorges Reservoir and panorama view of the slope in 2018

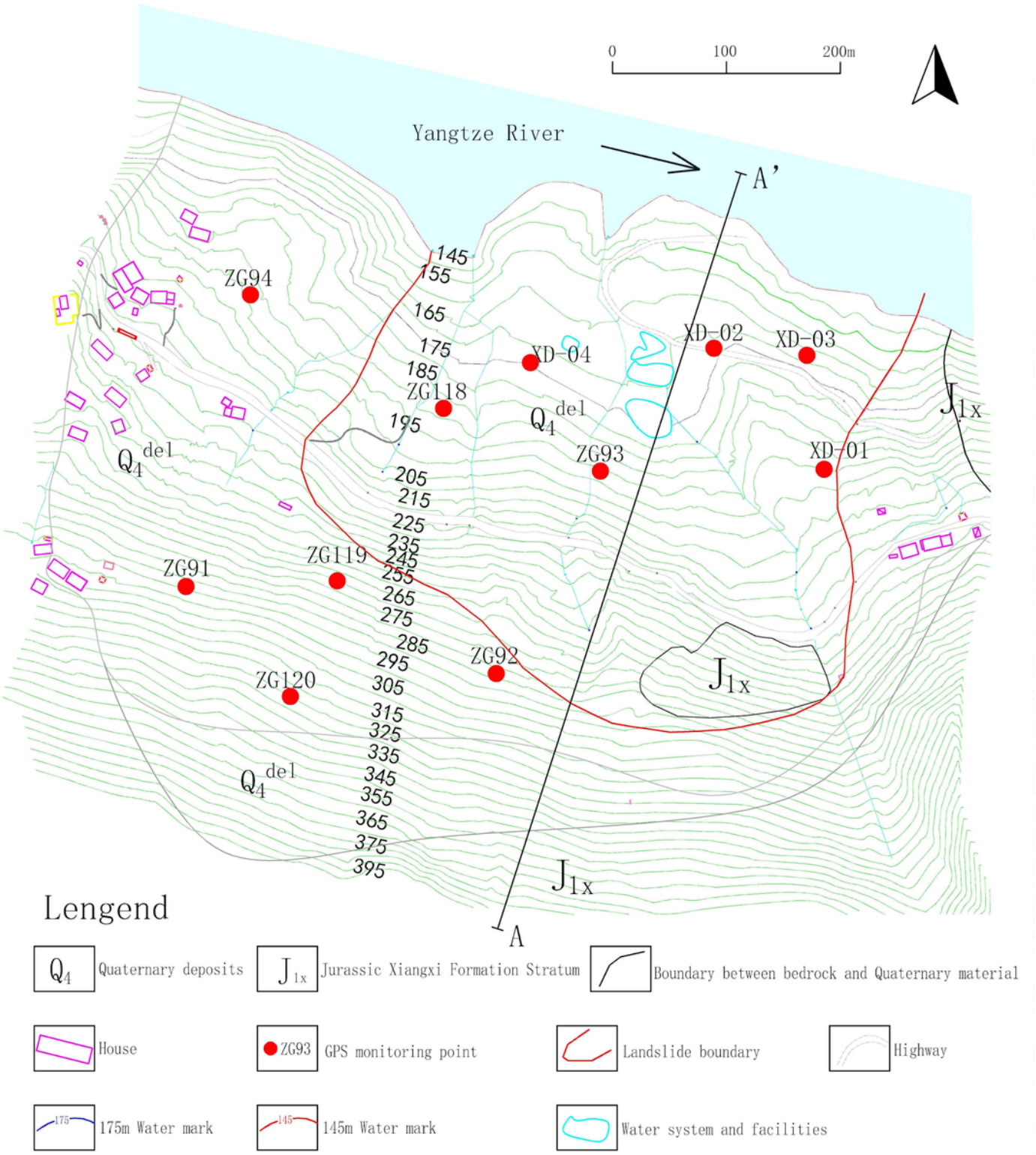

Figure 7

Geomorphic map of Baishuihe landslide

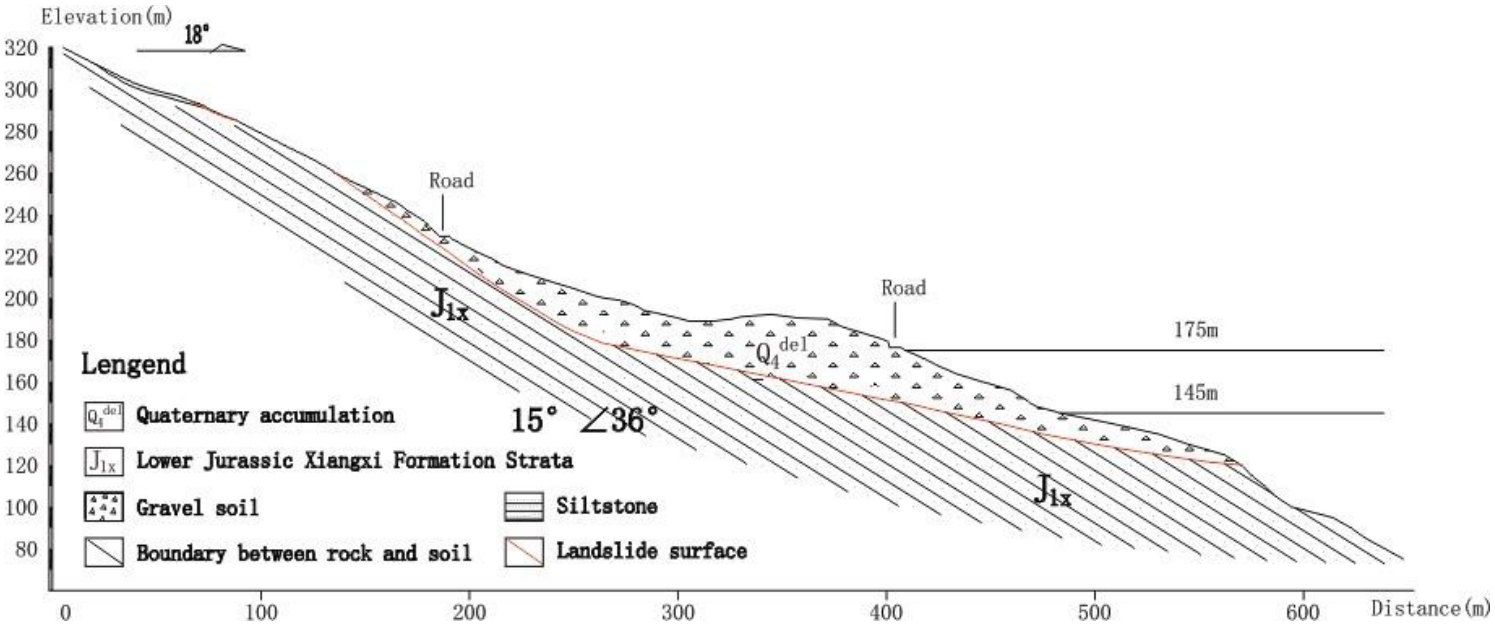

Figure 8

Cross section (A-A') of Baishuihe landslide

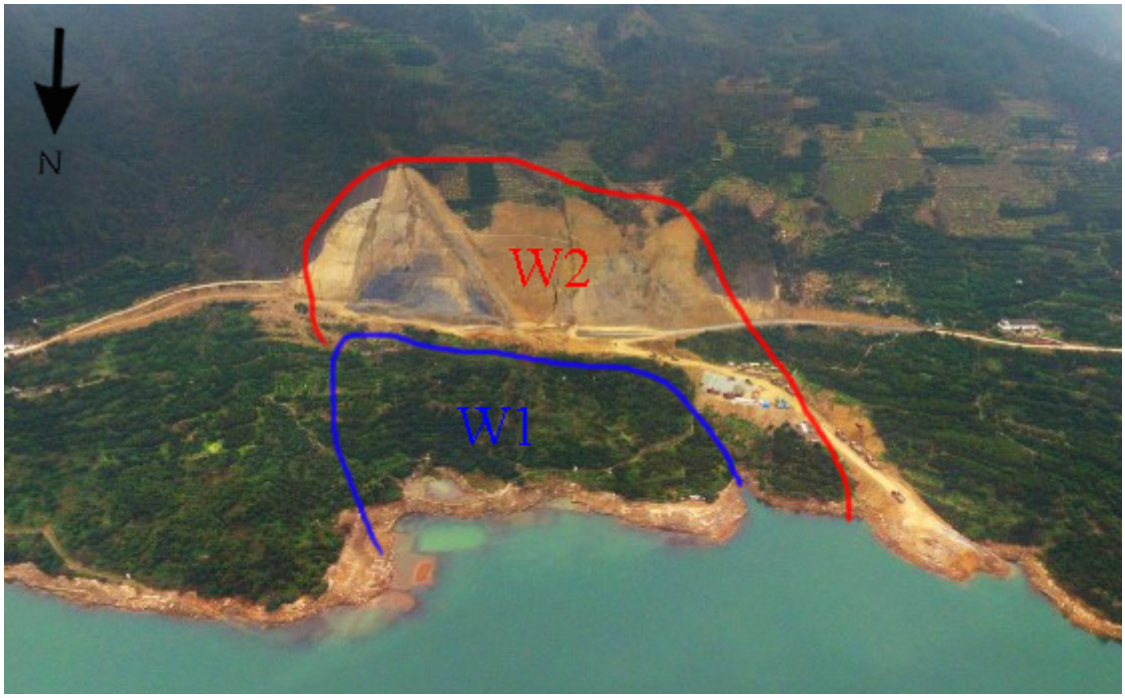

Figure 9

Panorama image by UAV of Stabilization construction in progress

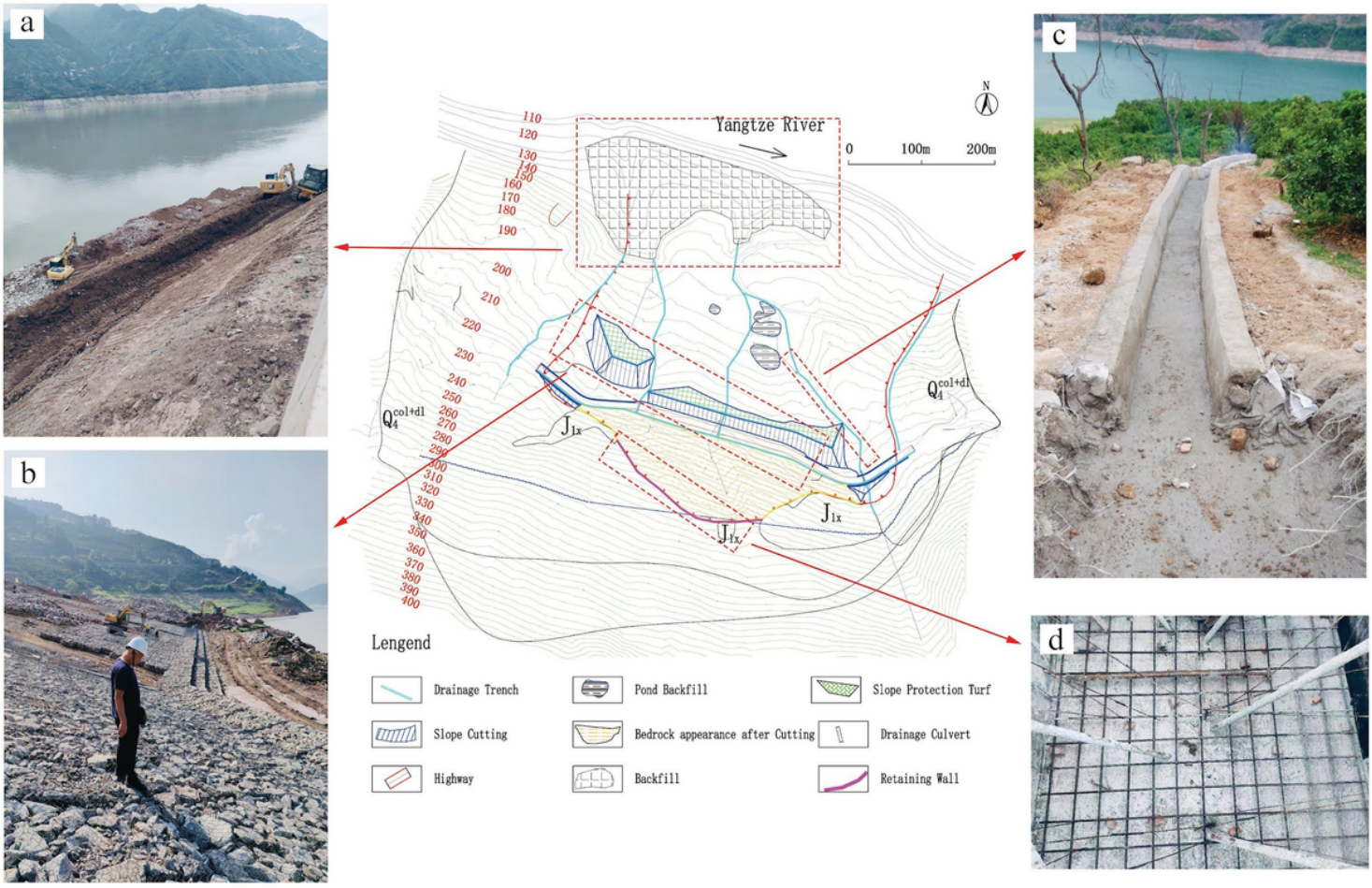

Figure 10

Stabilization measures on Baishuihe landslide

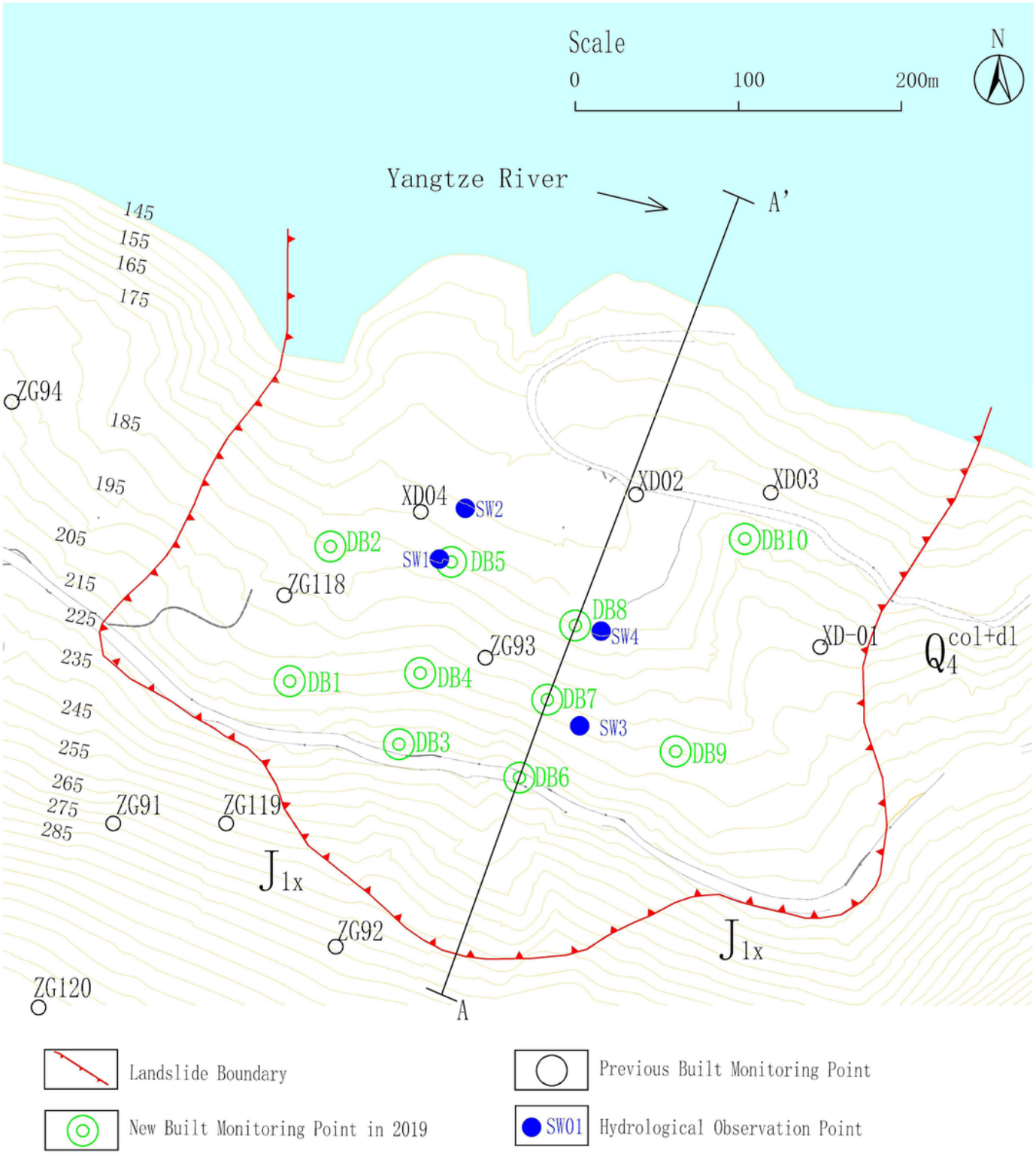

Figure 11

Layout of monitoring stations after stabilization works

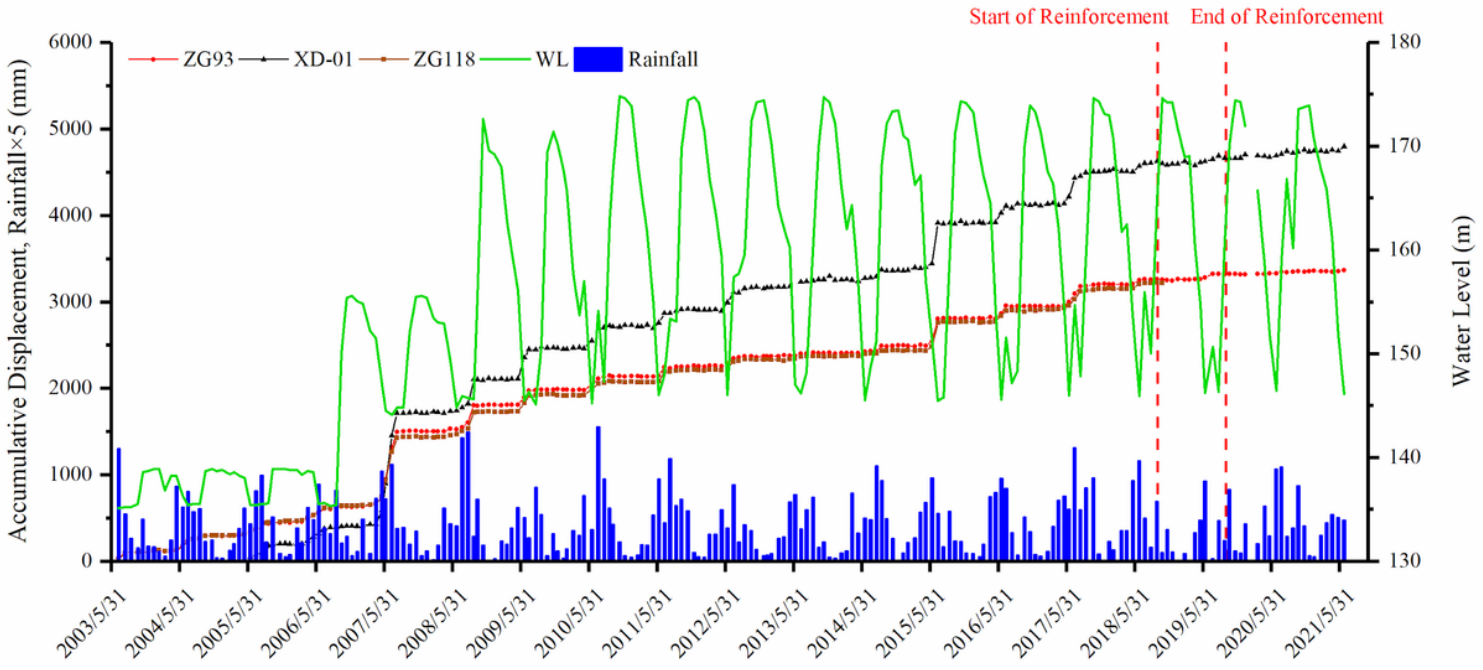

Figure 12

Monthly rainfall, accumulative displacement in some landslide positions, and reservoir water level from 2003 to 2021

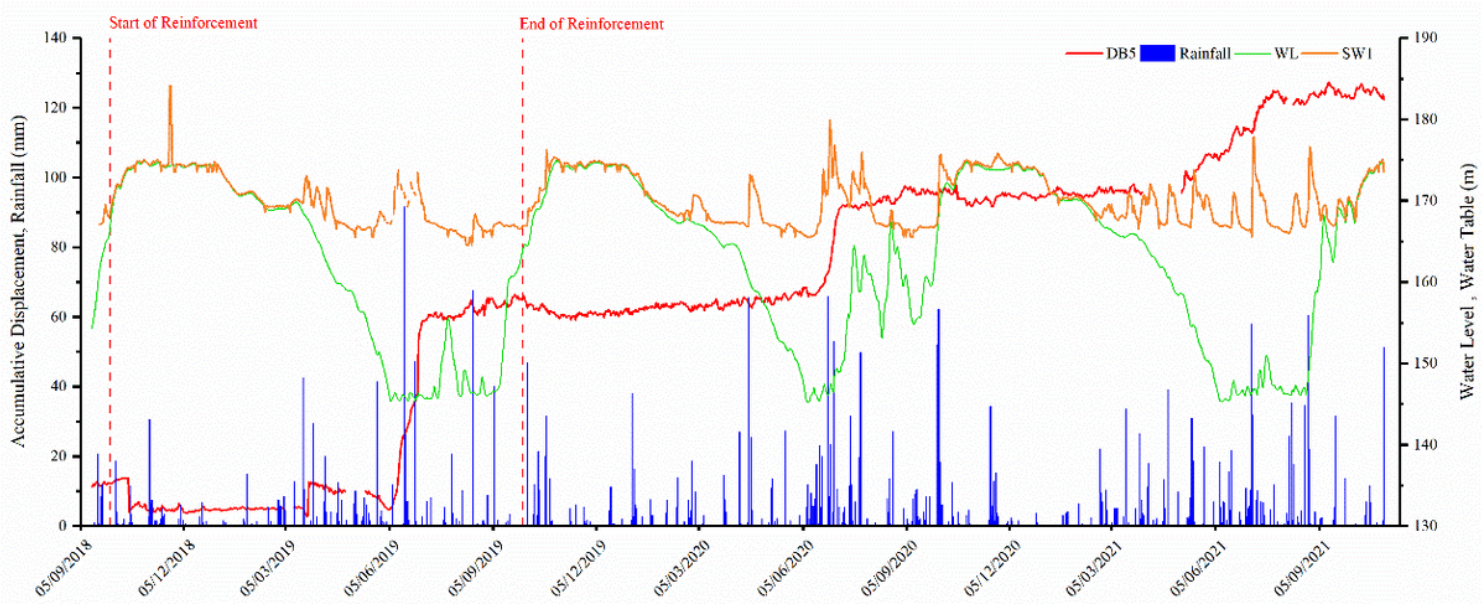

Figure 13

Daily rainfall, accumulative displacement in DB5, reservoir water level and water table in one piezometer from the stabilization work beginning

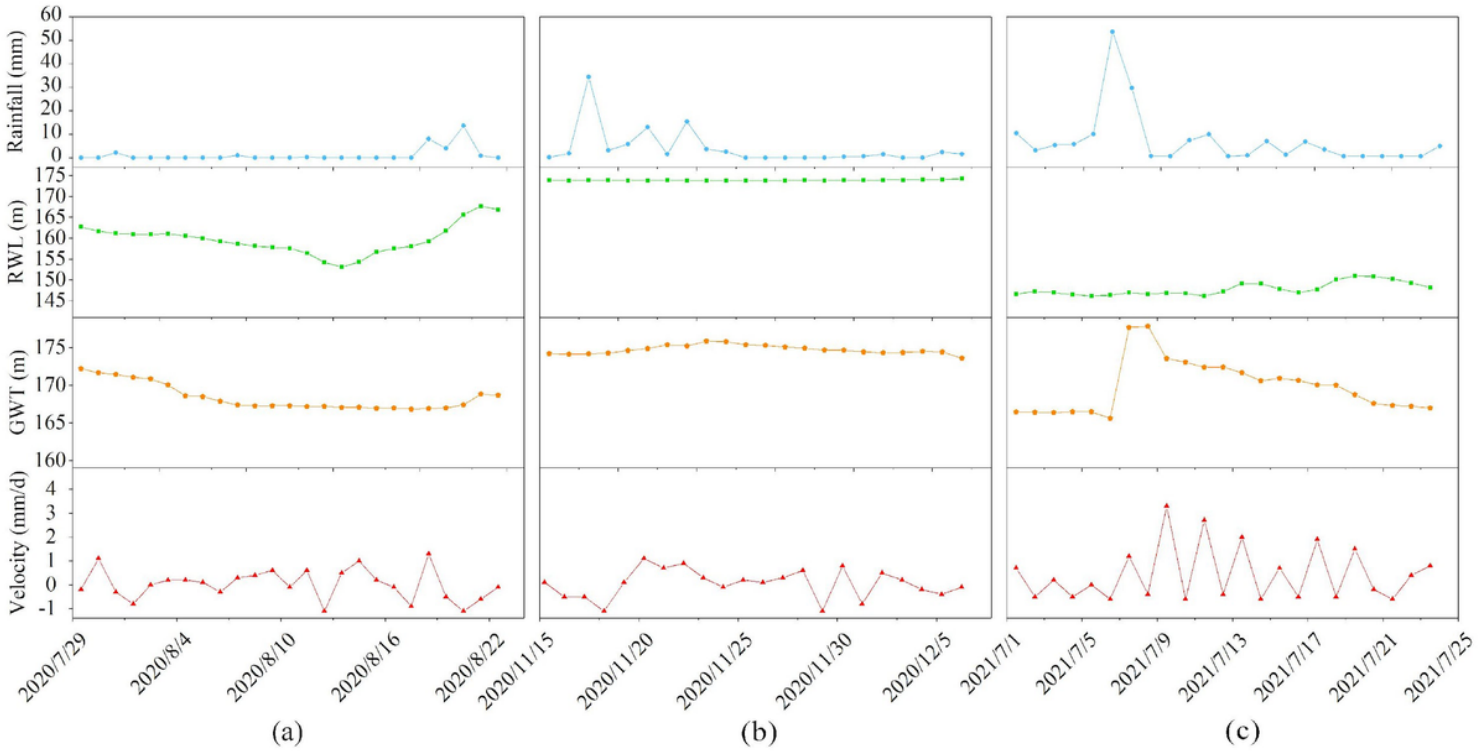

Figure 14

Three typical situations of heavy rainfall in a short period with different reservoir water levels

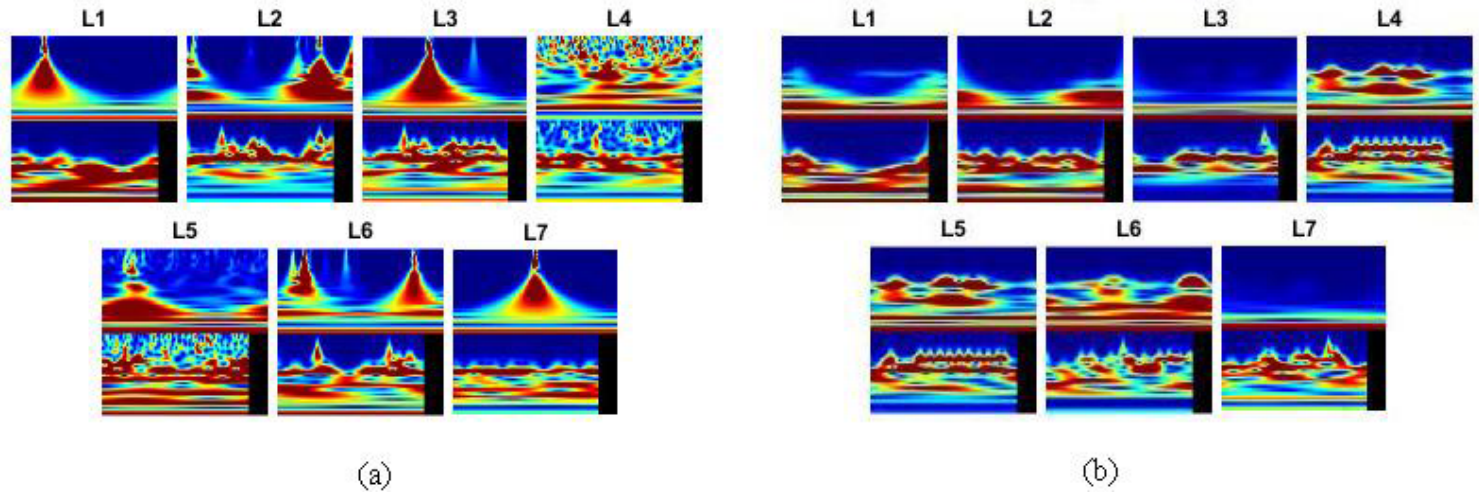

Figure 15

CNN Input Images with V-Single Factor Scalograms for Seven Highlighted Events

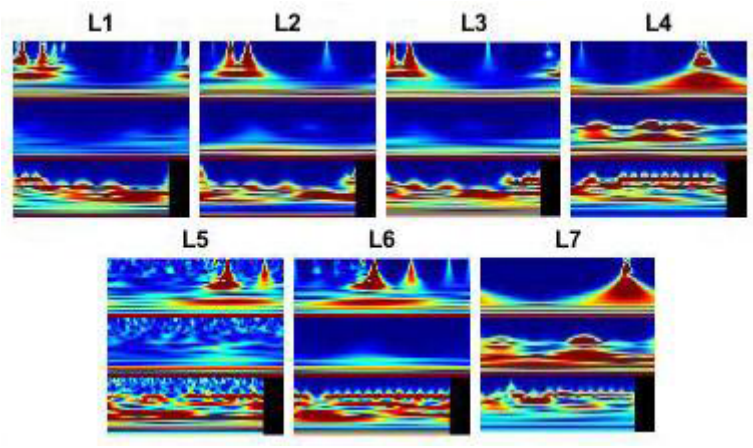

Figure 16

CNN Input Images with V-R-ΔW Factors Scalograms for Seven Highlighted Events

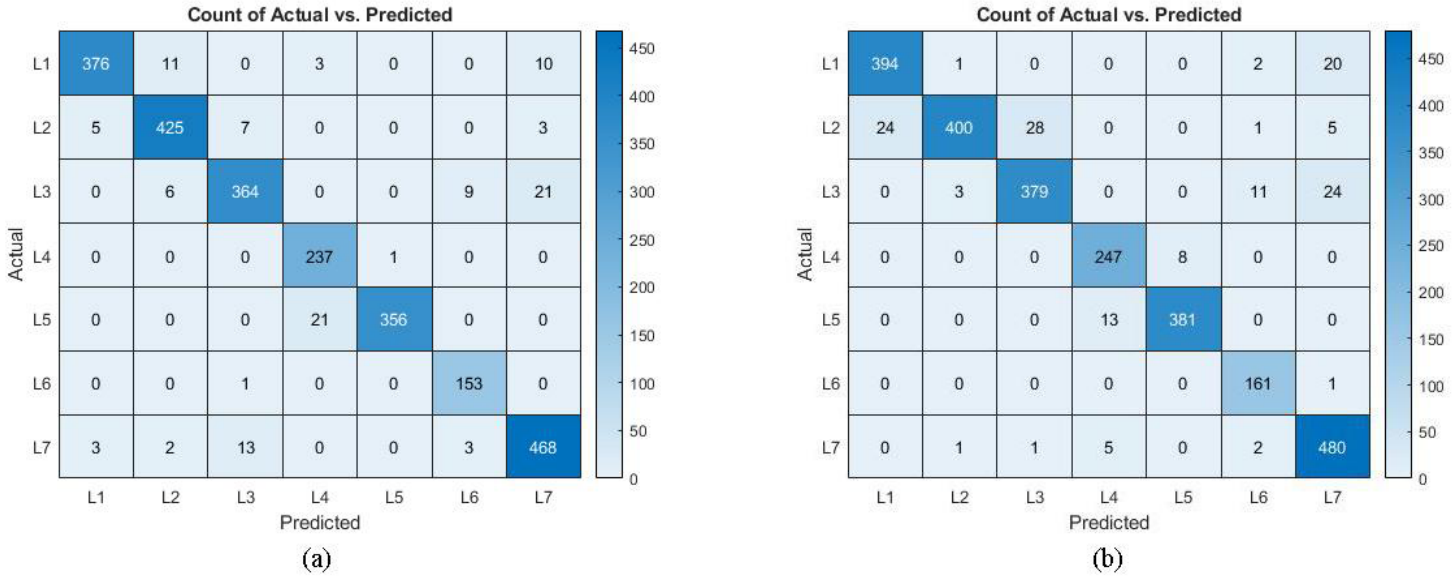

Figure 17

Confusion Matrices of tests with R-V and ΔW-V Scalograms

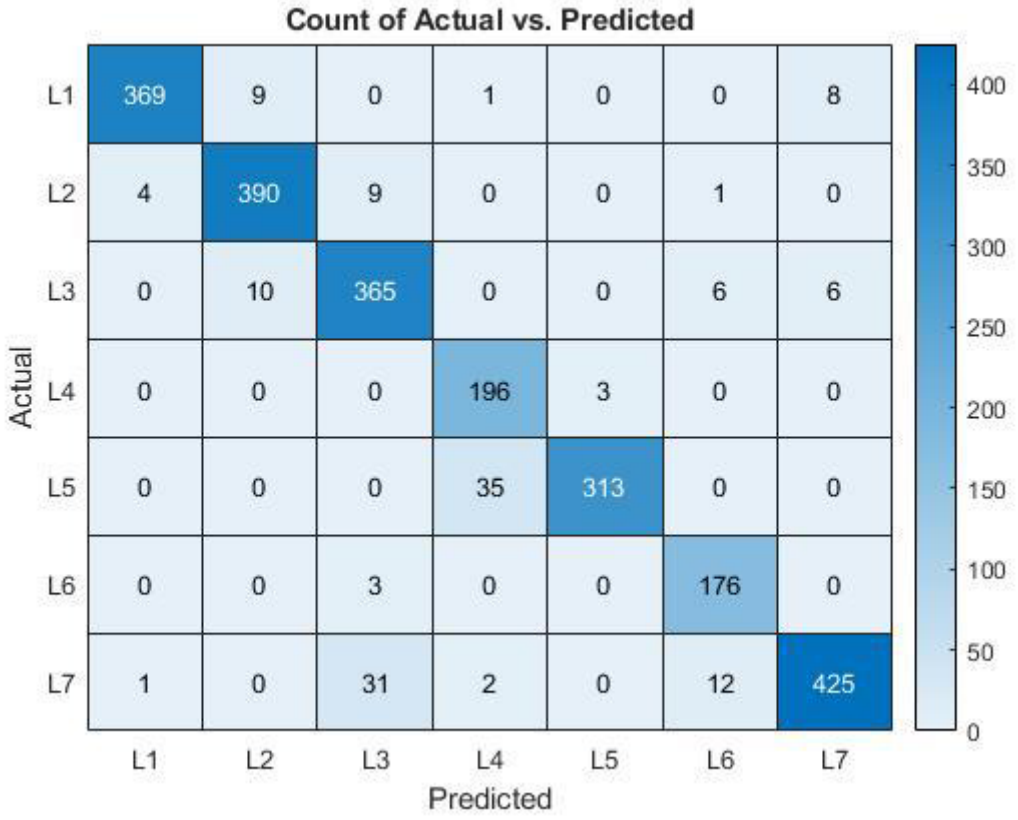

Figure 18

Confusion Matrix of test on V-R-ΔW Scalograms

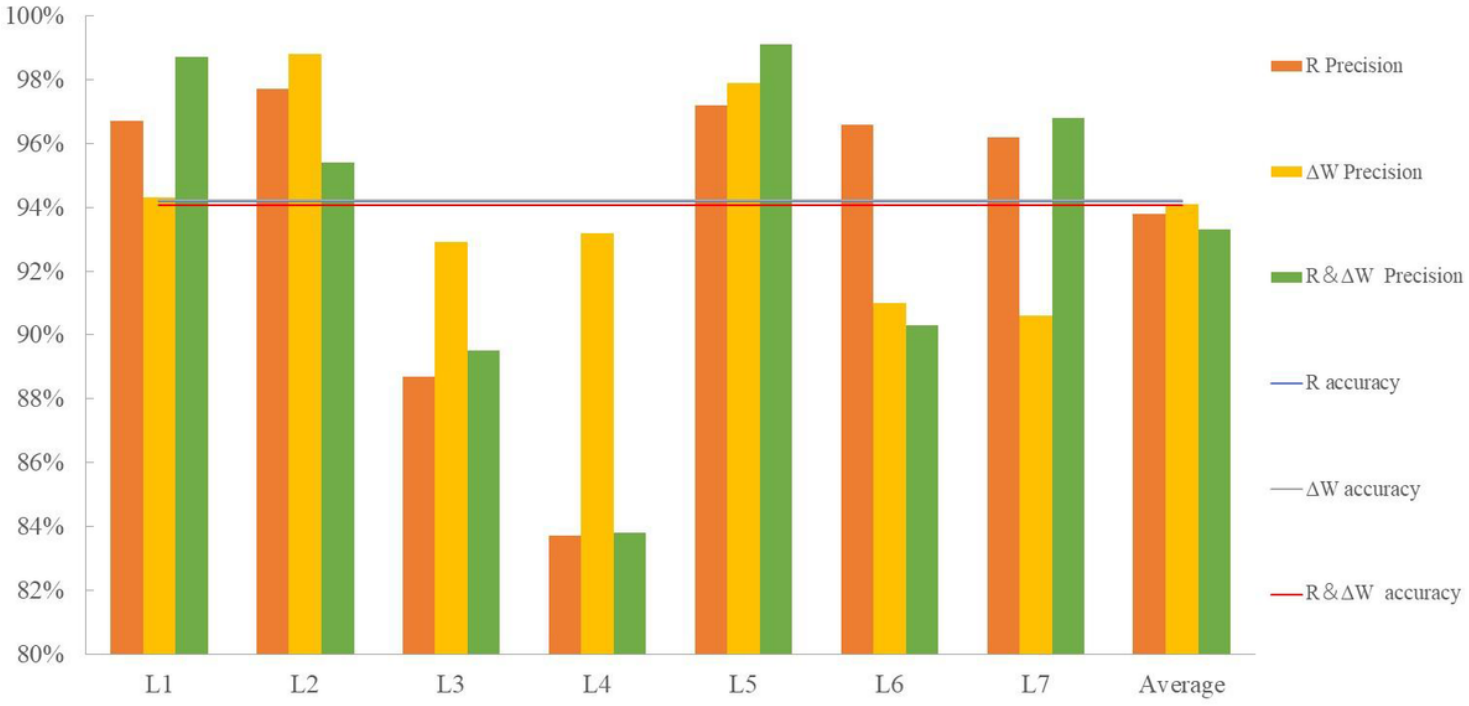

Figure 19

Comparison among three configurations of CNN-trained scalograms